Heliyon 10 (2024) e27172

Contents lists available at ScienceDirect

Heliyon

journal homepage: www.cell.com/heliyon

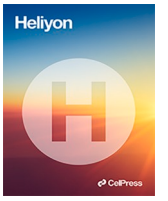

Research article

CLEC4E upregulation in gastric cancer: A potential therapeutic target correlating with tumor-associated macrophages

Qin Jiang [a], Dan Xiao [a], Ao Wang [a], Qiong Yu [a], Ying Yin [a], Jingchong Wu [a], Yan Zhang [a], Tian Jin [b], Baicheng Kuang [c,**], Yegui Jia [a,*]

[a] Department of Gastroenterology, The Sixth Hospital of Wuhan, Affiliated Hospital of Jianghan University, Wuhan, 430000, China
[b] Department of Pathology, Hanchuan People's Hospital, Hanchuan, 431600, China
[c] Institute of Organ Transplantation, Tongji Hospital, Tongji Medical College, Huazhong University of Science and Technology, Wuhan, 430030, China

ARTICLE INFO

Keywords:
CLEC4E
Gastric cancer
Tumor-associated macrophages
Stigmasterol

ABSTRACT

Background: CLEC4E has been reported to promote lung cancer progression. Tumor-associated macrophages (TAMs) play an important role in tumorigenesis. Whether the expression of CLEC4E in TAMs is associated with gastric carcinogenesis remains unclear.
Methods: The TIMER, UALCAN, UCSC Xena, and KM plotter databases are used to examine the expression of CLEC4E and its prognostic significance in gastric cancer (GC). Additionally, GO, KEGG, and GSEA analysis were conducted, and single-cell RNA-seq (scRNA-seq) datasets were utilized. The Coremine medical database was used to predict therapeutic drugs, and molecular docking was performed. Human GC samples were obtained, and co-culture models were constructed to evaluate the effects of CLEC4E in TAMs on tumor growth, migration, and invasion *in vitro*.
Results: CLEC4E was significantly upregulated in GC, and high CLEC4E expression was associated with poor prognosis. Western blotting and immunostaining showed increased protein levels of CLEC4E in GC. GO, KEGG, and GSEA results indicated that CLEC4E is involved in immune response. Immune infiltration analysis demonstrated that CLEC4E expression positively correlated with multiple immune cell types. scRNA-seq analyses revealed that CLEC4E was predominantly expressed in myeloid cells specifically TAMs, in GC. *In vitro* experiments confirmed that MFC induced CLEC4E expression in TAMs to mediate tumor progression. Specifically targeting CLEC4E by si-CLEC4E or stigmasterol inhibited cancer cell migration and invasion.
Conclusion: CLEC4E is a potential prognostic biomarker and new therapeutic target for GC that can be specifically targeted by stigmasterol.

1. Introduction

Gastric cancer (GC) is a malignant tumor that develops in the epithelium of the gastric mucosa in the digestive system, predominantly forming gastric adenocarcinoma. It ranks fifth among the most common malignant cancers worldwide, and is the third leading

* Corresponding author.
** Corresponding author.
E-mail addresses: d202282098@hust.edu.cn (B. Kuang), jyg218@sina.com (Y. Jia).

https://doi.org/10.1016/j.heliyon.2024.e27172
Received 15 August 2023; Received in revised form 22 February 2024; Accepted 26 February 2024
Available online 28 February 2024

Abbreviations

BMDMs	Bone marrow–derived macrophages
CLEC4E	C-Type Lectin Domain Family 4 Member E
EDU	5-Ethynyl-2′-deoxyuridine
GC	Gastric cancer
GO	Gene Ontology
GSEA	Gene Set Enrichment Analysis
H&E	Hematoxylin and eosin
IF	Immunofluorescence
KEGG	Kyoto Encyclopedia of Genes and Genomes
scRNA-seq	Single-cell RNA-seq
STAD	Stomach adenocarcinoma
TAMs	Tumor-associated macrophages
TCGA	The Ca-ncer Genome Atlas
TIMER	Tumor Immune Estimation Resource

cause of cancer-related deaths globally [1,2]. Despite some improvements in diagnosis and treatment, the prognosis of patients with GC remains poor [3,4]. Since the early symptoms of GC are insidious, most patients are diagnosed in the advanced stages [5,6]. Therefore, there is an urgent need to identify effective prognostic biomarkers and explore new therapeutic targets to improve the clinical outcomes of patients with GC.

The tumor microenvironment (TME) is composed of immune cells, tumor cells, and their metabolic products and plays an important role in the development of gastric cancer [7,8]. Tumor-associated macrophages (TAMs), one of the main stromal cells that compose the TME, are reported to be able to promote cancer progression [9,10]. C-type lectins are protein superfamilies that bind to microbial glycans and are important pattern recognition receptors in the innate immune system [11]. Among these, the C-type lectin domain family 4 member E receptor (CLEC4E, also called Mincle) is predominantly expressed by macrophages and can be activated during both bacterial infection [12,13] and sterile inflammation, such as cisplatin-induced acute kidney injury [14]. Recent studies have shown that the C-type lectin domain family 4 member A (CLEC4A) and L receptors (CLEC4L) are significantly upregulated in liver cancer and are closely related to the infiltration of immune cells [15], and CLEC4E expression is essential for TAMs to promote lung cancer progression [16]. However, the effects of CLEC4E on gastric carcinogenesis and immunocyte infiltration in the TME remain unclear and require further exploration.

Based on bioinformatics analysis, biological experiments, and network pharmacology techniques, we explored the expression, prognosis, and immune infiltration of CLEC4E in GC. Through scRNA-seq analyses and immunofluorescence staining, we confirmed that CLEC4E is predominantly expressed in TAMs in GC. By regulating CLEC4E expression in TAMs, we investigated the effects of CLEC4E in the TME on GC progression. In addition, we predicted and verified potential therapeutic drugs for CLEC4E. The results showed that stigmasterol binds to CLEC4E with high affinity and exerts tumor-suppressive effects by downregulating CLEC4E in TAMs.

2. Material and methods

2.1. Gene expression analysis

The mRNA levels of CLEC4E in pan-cancers were visualized using the Tumor Immune Estimation Resource (TIMER) database (https://cistrome.shinyapps.io/timer/) [17]. The expression data for CLEC4E in GC (stomach adenocarcinoma (STAD) were downloaded from The Cancer Genome Atlas (TCGA) and the UCSC Xena database (https://xenabrowser.net/datapages/) [18]. Differential expression of CLEC4E between disease states (normal or tumor) and cancer stages (normal or grade 1–3) of GC was analyzed using UALCAN (http://ualcan.path.uab.edu/) and represented as box plots. R (version 4.2.1) was used to draw paired sample wiring plots.

2.2. Kaplan–Meier plotter analysis

An online Kaplan–Meier plotter (https://kmplot.com/analysis/) was used to analyze the prognostic value of CLEC4E in patients with GC. Data from 875 patients with GC were analyzed. Patients were divided into low- and high-expression groups based on the median expression of CLEC4E (probe set 219859_at). These two groups were then compared using overall survival (OS), and a K–M survival plot was generated. In addition, the relationship between CLEC4E expression and patient prognosis in relation to the immune cell subpopulation was analyzed. The log-rank p-values and hazard ratios (HR) were calculated. To evaluate the predictive power of CLEC4E, the "timeROC," "ggplot2" R packages were used to conduct the receiver operating characteristic (ROC) curve.

2.3. Functional enrichment analysis

To explore the biological functions of CLEC4E in GC, we utilized the top 300 genes that were positively and negatively coexpressed

with CLEC4E for Gene Ontology (GO) and Kyoto Encyclopedia of Genes and Genomes (KEGG) Pathway Enrichment Analysis separately, employing the "ClusterProfiler" package. Gene Set Enrichment Analysis (GSEA) was used to explore the potential mechanisms of the top 300 genes that were positively coexpressed with CLEC4E.

2.4. CLEC4E-interacting genes analysis

A correlation analysis of CLEC4E and other genes in GC was performed, and the top 10 genes positively or negatively associated with it were presented in the form of heat maps. The GeneMANIA database (http://www.genemania.org) was used to construct an interaction network between the genes and CLEC4E.

2.5. Immune cell infiltration analysis

The TIMER database was used to explore the relationship between CLEC4E expression and levels of tumor immune cell infiltration in patients with GC. The results were displayed as chordal plots. In addition, the 24 immune cells correlated with CLEC4E expression were further analyzed using the GSVA R package (https://bioconductor.org/packages/devel/bioc/html/GSVA.html) in GC and presented using lollipop.

2.6. Single-cell sequencing (scRNA-seq) analysis

scRNA-seq data for STAD (GSM5004181) were downloaded from the GEO database. The "Seurat" package was used for data integration and quality control, UMAP algorithms were applied for the dimensionality reduction, cells were clustered together by FindClusters, and the expressions of CLEC4E in different cell clusters were visualized by "Vlnplot" package [19].

2.7. Collection of patient samples

Six GC specimens and six normal gastric tissues adjacent to the tumors were collected from the Sixth Hospital of Wuhan, Affiliated Hospital of Jianghan University, China. The specimens were divided and were either stored at −80 °C or fixed in 4% formaldehyde and paraffin-embedded for further assays. The study was conducted in accordance with the Declaration of Helsinki and approved by the Ethics Committee of the Sixth Hospital of Wuhan (CREC Ref. No.: WHSHIRB-K-2023010). Written informed consent was obtained from all patients.

2.8. Animals

Male C57BL/6J mice (4–6 weeks old) were purchased from Beijing Vital River Laboratory Animal Technology Co., Ltd. (Beijing, China). Animals were maintained under a specific pathogen-free environment, with a constant 12-h light-dark cycle and 25 °C and 55% relative humidity, free access to food and water. All animal experiments were performed in accordance with the guidelines of the Chinese Council on Animal Care and approved by the Animal Ethics Experimental Committee (CREC Ref. No.: WHSHIRB-K-2023010).

2.9. Reagents and antibodies

Antibodies against human CLEC4E (ab100846), CD68 (ab303565) were obtained from Abcam (Cambridge, UK), rabbit *anti*-CLEC4E (A20156) was purchased from ABclonal (Wuhan, China), β-actin (60008-1-Ig) were provided by Proteintech (Rosemont, PA, USA). The nuclear dye 4′,6-diamidino-2-phenylindole (DAPI, D8417) and dimethyl sulfoxide (DMSO, W387520) were offered by Sigma-Aldrich (St. Louis, MO, USA). Penicillin, streptomycin, fetal bovine serum (FBS) and DMEM/F12 were purchased from Gibco (Carlsbad, CA, USA). Stigmasterol (HY–N0131) and Beta-sitosterol (HY–N0171A) were purchased from MedChemExpress (MCE) (New Jersey, USA).

2.10. Hematoxylin and eosin (H&E) staining

Paraffin-embedded gastric mucosal tissues were sliced into 5-μm-thick sections and stained with H&E, in accordance with the manufacturer's instructions. Briefly, after deparaffinization and rehydration, the sections were stained with H&E, dehydrated with graded alcohol, and cleaned with xylene. The images were acquired using an Olympus BX-51 microscope (Tokyo, Japan).

2.11. Immunofluorescence (IF)

To confirm whether CLEC4E was expressed in TAMs, double IF staining for CD68 and CLEC4E was performed as previously described [20]. The deparaffinized and rehydrated gastric mucosa sections underwent antigen retrieval, and were blocked by 10% bovine serum albumin (BSA) for 1 h at 37 °C. Following this, the sections were incubated with primary antibodies overnight at 4 °C. The primary antibodies used were CD68 (Abcam, ab303565, 1:50) and CLEC4E (Abcam, ab100846, 1:100). Subsequently, Alexa Fluor 594-conjugated donkey anti-rabbit IgG (H + L) (Life Technologies, A21207, 1:400) and Alexa Fluor 488-conjugated donkey anti-mouse IgG (H + L) (Life Technologies, A21202, 1:400) were used as secondary antibodies. The sections were viewed and

photographed using a fluorescence microscope (ECLIPSE C1; NIKON, Tokyo, Japan). Six field images per animal were randomly selected to calculate the average number of CD68/CLEC4E-positive cells.

2.12. Cell culture

The murine GC cell line mouse forestomach carcinoma MFC (CL-0156) was purchased from Procell Life Science & Technology Co., Ltd. (Wuhan, China). Cells were cultured in DMEM/F12 medium with 10% FBS and 1% penicillin and streptomycin at 37 °C in a humidified incubator with 5% CO_2. Cancer-conditioned medium was collected as described previously [16]. After serum-starved for 24 h, the MFC cells culture medium (MFC-CM) was collected, centrifuged (500×*g*, 4 °C, 10 min) and filtered by a 0.22 μm membrane sterile filter. Then, they were stored at −80 °C for the following co-culture experiments.

2.13. Isolation and culture of primary bone marrow cells

To obtain bone marrow-derived macrophages (BMDMs), bone marrow cells were harvested from femurs and tibias of 4–6-week-old C57BL/6J mice as previously described [21]. Subsequently, cells were cultured in DMEM/F12 medium with 10% FBS and 20 ng/mL macrophage colony-stimulating factor (M-CSF, PeproTech, London, UK) in 5% CO_2 at 37 °C to induce the formation of BMDMs. After 7 d of culture, the induced BMDMs were harvested. To obtain TAMs, BMDMs were treated with 10% MFC-CM in DMEM/F12 (MFC-CM group). For drug experiments, different concentrations of stigmasterol (10, 20 μmol/L) or Beta-sitosterol (13, 26 μmol/L) were added to the medium 24 h before 10% MFC-CM stimulation as previously described.

2.14. Cell transfection of siRNA

For knockdown assay *in vitro*, siRNAs targeting CLEC4E (si-CLEC4E-1, sense 5′-CCUUUGAACUGGAAACAUUTT-3′, antisense 5′-AAUGUUUCCAGUUCAAAGGTT-3′; si-CLEC4E-2, sense 5′-CAUCACCAGAUGUGUCGUAACAUAU-3′, antisense 5′-AUAUGUUACGACACAUCUGGUGAUG-3′; si-CLEC4E-3, sense 5′-CCUGUUUCUACAGUAUGCCUUGGAU-3′, antisense 5′-AUCCAAGGCAUACUGUAGAAACAGG-3′) and nonsense control siRNA (si-NC, 5′-sense: UUCUCCGAACGUGUCACGUTT-3′, antisense: 5′-ACGUGACACGUUCGGAGAATT-3′) were used (Hanbio, Shanghai, China). According to the manufacturer's instruct-ions, 100 pmol of si-NC or si-CLEC4E were transfected into BMDMs with L-ipo8000™ (C0533, Beyotime) 24 h prior to experiments. Fluorescence imaging and Western blot assays were performed to assess transfection efficiency.

2.15. Cell migration function assays

To investigate the effect of CLEC4E on TAM-mediated cancer progression, MFC cells (2×10^5 cells per well) were cultured in 12-well plates. After growing to 90% confluence, cells were serum-starved for 12 h and then cultured in 50% conditioned medium from MFC-CM-treated BMDMs (TAM-CM) or control media (BMDM-CM). The wound healing assay was conducted, and images were captured at 0 and 24 h after scratching. The transwell invasion assay was performed to evaluate cell invasion abilities as previously described [22]. Briefly, conditioned medium obtained from MFC-CM-stimulated BMDMs pretreated with si-CLEC4E, or si-NC was added into the lower chamber. MFC cells (2×10^4 per well) in serum-free medium were seeded into the upper chamber coated with 50 μL Matrigel. After co-incubation for 24 h at 37 °C, cells on the lower surface of the chamber were fixed with 4% paraformaldehyde and stained with 0.1% crystal violet. Each assay was independently conducted three times, and images were acquired using an Olympus BX-51 microscope (Tokyo, Japan). ImageJ software was used to calculate the mean cell migration area and number of migrated cells.

2.16. Cell proliferation assay and 5-Ethynyl-2′-deoxyuridine (EdU) staining

Cell viability experiments were conducted using a CCK-8 kit (Beyotime, China) according to the manufacturer's instructions. Briefly, MFC were seeded in 96-well plates at 2000 cells per well for 12 h before si-NC or si-CLEC4E treatment. Forty-80 h post-transfection, 20 μl of CCK-8 was added and incubated with cells for 1 h at 37 °C. Subsequently, the absorbance was measured at 450 nm. The viability of cells in the si-NC group was normalized to 100%. In addition, after co-culture with TAM-CM for 24 h, MFC were subjected to EdU staining assays using an EdU-488 cell proliferation detection kit (Beyotime, C0071S), following the manufacturer's protocol. Images were obtained using a fluorescence microscope (ECLIPSE C1; NIKON, Tokyo, Japan).

2.17. Western blot

Total protein from gastric mucosal homogenates or cultured cells was extracted using a Cell Lysis Buffer (P0013J, Beyotime), and the BCA Protein Assay Kit (P0010S, Beyotime) was used for protein quantification. 40 μg of protein were added per hole and separated by 4%–20% SDS-PAGE and then transferred to 0.45 μm PVDF membranes (Millipore). Membranes were blocked in 5% skim milk at normal temperature for 1 h and incubated with the primary antibodies (CLEC4E, 1:1000) overnight at 4 °C followed by the second antibody incubation. The β-actin was used as an internal control. The protein bands were photographed using the GeneGnome XRQ system (Syngene, Cambridge, UK) and analyzed using ImageJ software (NIH, MD, USA).

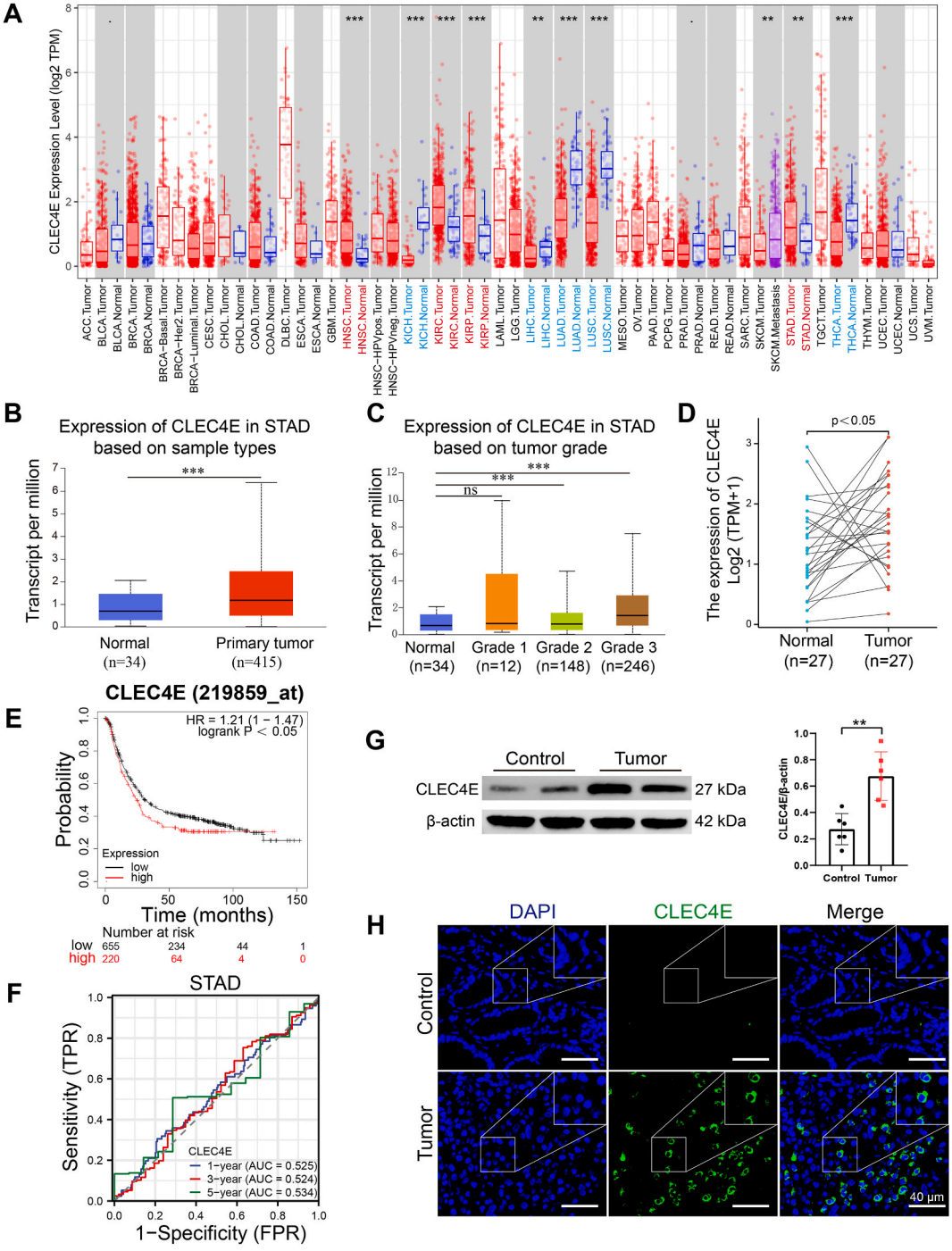

Fig. 1. Expression and survival analysis of CLEC4E in GC. (**A**) Different expression of CLEC4E in pan-cancer investigated with the TIMER database. (**B**) CLEC4E expression in GC compared to normal tissues and (**C**) among different cancer stages using the UALCAN database. (**D**) CLEC4E expression in 27 pairs of GC tissues and adjacent normal tissues. (**E**) Prognostic analysis of CLEC4E expression with OS in GC patients using KM plotter. (**F**) AUC of ROC curve verified the prognostic power of CLEC4E expression in the TCGA cohort. (**G**) Western blot for CLEC4E protein in normal control and GC tissues and quantitative analysis (n = 6). The original blots are shown in Supplementary Fig. S1. (**H**) Representative IF staining of CLEC4E protein (green). Data represented by mean ± SD. *p < 0.05, **p < 0.01; ns indicates no significance. (For interpretation of the references to color in this figure legend, the reader is referred to the Web version of this article.)

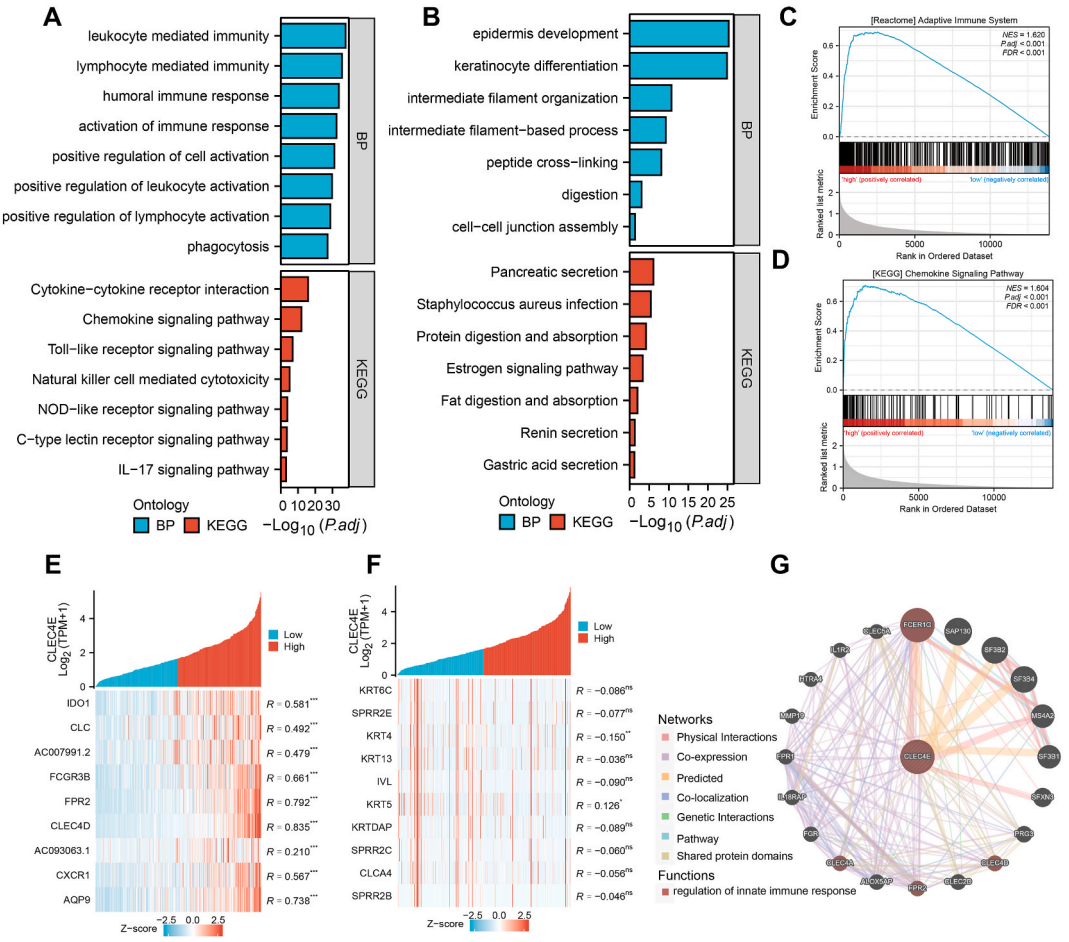

Fig. 2. CLEC4E expression in GC was closely related to the immune response in the TME. (**A**) Enrichment analyses of the top 300 genes positively coexpressed with CLEC4E in GC. (**B**) Enrichment analyses of the top 300 genes negatively coexpressed with CLEC4E in GC. (**C-D**) Representative GSEA pathways enriched in samples with high CLEC4E expression. (**E-F**) Top 9–10 genes positively (**E**) or negatively (**F**) correlated with CLEC4E expression in GC. (**G**) The gene-gene interaction network of CLEC4E constructed by GeneMania. Data represented by mean ± SD. *p < 0.05, **p < 0.01, ***p < 0.001, ns indicates no significance.

2.18. Potential drug prediction and molecular docking

The Coremine medical database (https://coremine.com/medical/#search) was used for screening traditional Chinese medicine (TCM) with potential properties targeting CLEC4E. The traditional Chinese medicine systems pharmacology database and analysis platform (TCMSP) (https://www.tcmsp-e.com/tcmsp.php) was used to screen the corresponding active ingredients of TCMs based on specific screening criteria including, oral bioavailability (OB) ≥30% and drug likeness (DL) ≥0.18. The VENNY tool (https://bioinfogp.cnb.csic.es/tools/venny_old/) was used to identify the ingredients that may play a major role in targeting CLEC4E. Molecular docking was performed to explore the interactions between CLEC4E and stigmasterol or Beta-sitosterol. The 2D structure of the small molecules was downloaded from PubChem (https://pubchem.ncbi.nlm.nih.gov/), and the PDB format file of CLEC4E (ID 3wh2) was downloaded from the RCSB PDB (https://www.rcsb.org/). ChemBio 3D, PyMOL, and Autodock Tools 1.5.6 were used to perform component-target docking, and Discovery Studio 2019 was used to display the results.

2.19. Statistical analysis

Statistical analyses were performed using the GraphPad Prism 8.0.1 (GraphPad Software, La Jolla, CA, USA). Data were presented as mean ± SD. Significance between two groups was determined using a two-tailed unpaired *t*-test, while one-way ANOVA was used for more than two groups. Pearson's correlation analysis was performed to determine the association between immune cell infiltration and CLEC4E expression. Survival analysis was performed using the log-rank test. Statistical significance was set at $P < 0.05$.

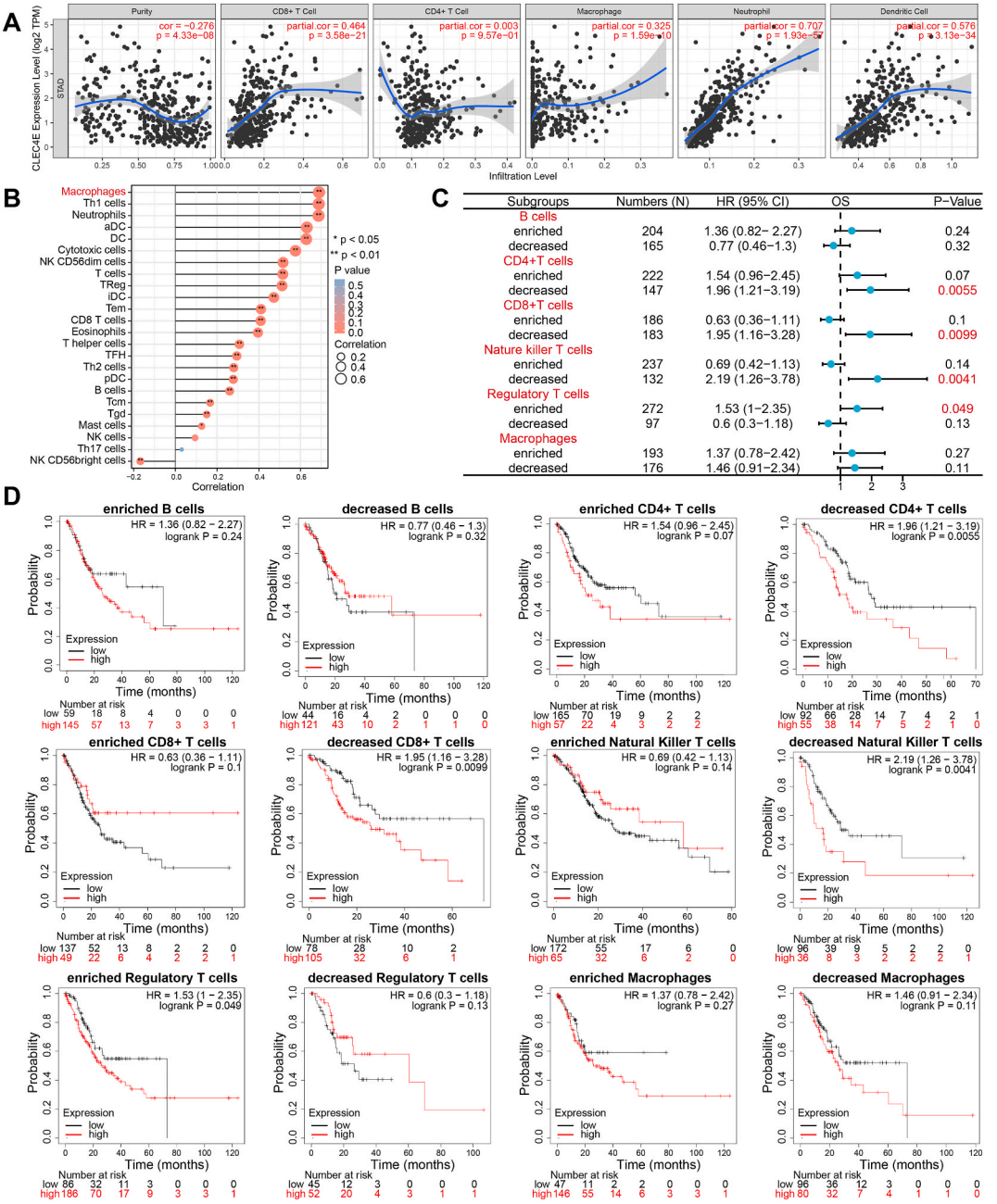

Fig. 3. Upregulated expression of CLEC4E was correlated with infiltrating immune cells in GC. (**A**) CLEC4E was positively correlated with the infiltration of different immune cells. (**B**) CLEC4E was correlated with several infiltrated immune cells in GC as displayed by a lollipop plot. (**C**) A forest plot shows the prognostic value of CLEC4E expression in different immune cell subgroups in GC. (**D**) Correlations between CLEC4E expression and OS in different subgroups of immune cell were estimated in GC patients using KM plotter. Data represented by mean ± SD. *p < 0.05, **p < 0.01, ns indicates no significance.

3. Results

3.1. CLEC4E expression is elevated with poor prognosis in GC

We initially evaluated the mRNA expression of CLEC4E in human multiple cancers using the TIMER database (Fig. 1A). Upregulation of CLEC4E was observed in GC tissues compared to normal gastric tissues. Moreover, CLEC4E expression was remarkably higher in HNSC, KIRC, and KIRP, whereas it was significantly lower in KICH, LIHC, LUAD, LUSC, and THCA than in the corresponding normal

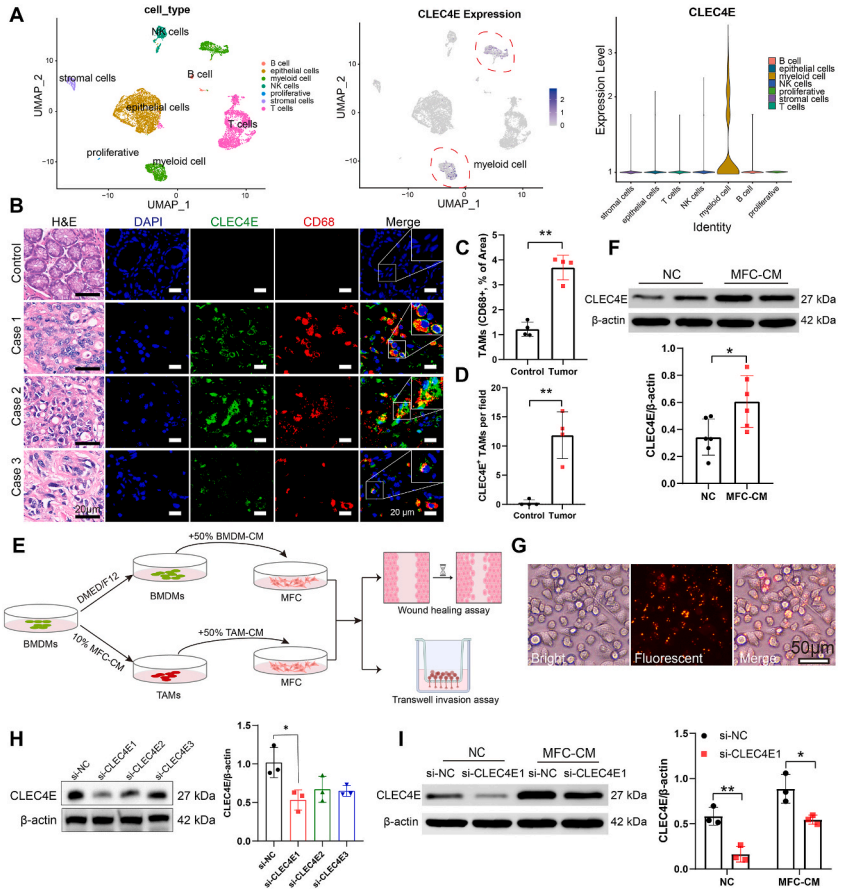

Fig. 4. TME induced CLEC4E expression in TAMs to mediated cancer progression. (**A**) scRNA-seq of an GC sample. UMAP plots of the cells sequenced here, colored by cell type (left), CLEC4E gene expression for cell type identification (blue, middle), Violin plots showing the expression of CLEC4E in the seven cell groups (right). (**B**) Representative micrographs of hematoxylin and eosin (H&E) and immunofluorescence staining of $CLEC4E^+$ TAMs ($CLEC4E^+$ & $CD68^+$) in normal and three GC patients with DAPI counterstain. (**C-D**) Quantitative analysis of TAMs and $CLEC4E^+$ TAMs (n = 4). (**E**) Schematic description of the experimental design for the follow-up studies. (**F**) Western blot for CLEC4E protein expression in BMDMs with or without MFC-CM treatment and quantitative analysis (n = 6). The original blots are shown in Supplementary Fig. S2A. (**G**) Representative image of Cy3-labeled siRNAs 24 h after transfection into BMDMs. (**H**) Western blot results of CLEC4E expression in BMDMs with different si-RNAs treatment and quantitative analysis (n = 3). (**I**) Western blot for CLEC4E expression in si-NC and si-CLEC4E pretreated BMDMs with or without MFC-CM stimulation 24 h before and quantitative analysis (n = 3). Original blots can be found in Supplementary Figs. S2B–C. Data represented by mean ± SD. *p < 0.05, **p < 0.01. (For interpretation of the references to color in this figure legend, the reader is referred to the Web version of this article.)

tissues, indicating that CLEC4E may play an important role in the progression of multiple cancers. Consistently, we found that CLEC4E was highly expressed in GC tissues compared to normal tissues in the UALCAN database (Fig. 1B). Further analysis of the tumor stage using the UALCAN online tool revealed higher CLEC4E expression in patients with GC at stages 2 and 3 (Fig. 1C). In addition, CLEC4E expression was significantly elevated in 27 GC samples compared to paired adjacent normal samples (Fig. 1D). Survival analysis revealed that GC patients with higher CLEC4E levels had worse OS ($P < 0.05$) (Fig. 1E). Time-dependent ROC curve (timeROC) analysis was performed to evaluate the predictive power of CLEC4E for the OS of patients with GC, and the area under the curve (AUC) at 1, 3, and 5-year reached 0.525, 0.524, and 0.534, respectively (Fig. 1F). To verify the expression pattern of CLEC4E in GC, tissue samples were collected from both GC and adjacent normal tissue. Western blot (n = 6, $p < 0.01$) and immunostaining results for CLEC4E revealed higher protein levels in GC tissues, consistent with the aforementioned results (Fig. 1G and H). Taken together, CLEC4E expression is elevated in patients with GC, and higher CLEC4E levels indicate an unfavorable prognosis.

3.2. GO, KEGG, and GSEA analysis of the coexpressed genes associated with CLEC4E in GC

To further explore the potential molecular functions of CLEC4E in GC, the mRNA expression data were downloaded from the UCSC Xena browser. Based on the median CLEC4E expression, 375 patients with GC were divided into high and low CLEC4E expression groups. To explore the pathways and biological functions associated with CLEC4E, GO and KEGG enrichment analyses were conducted on the top 300 genes that positively or negatively coexpressed with CLEC4E, separately (Fig. 2A and B). In terms of BP, upregulation of

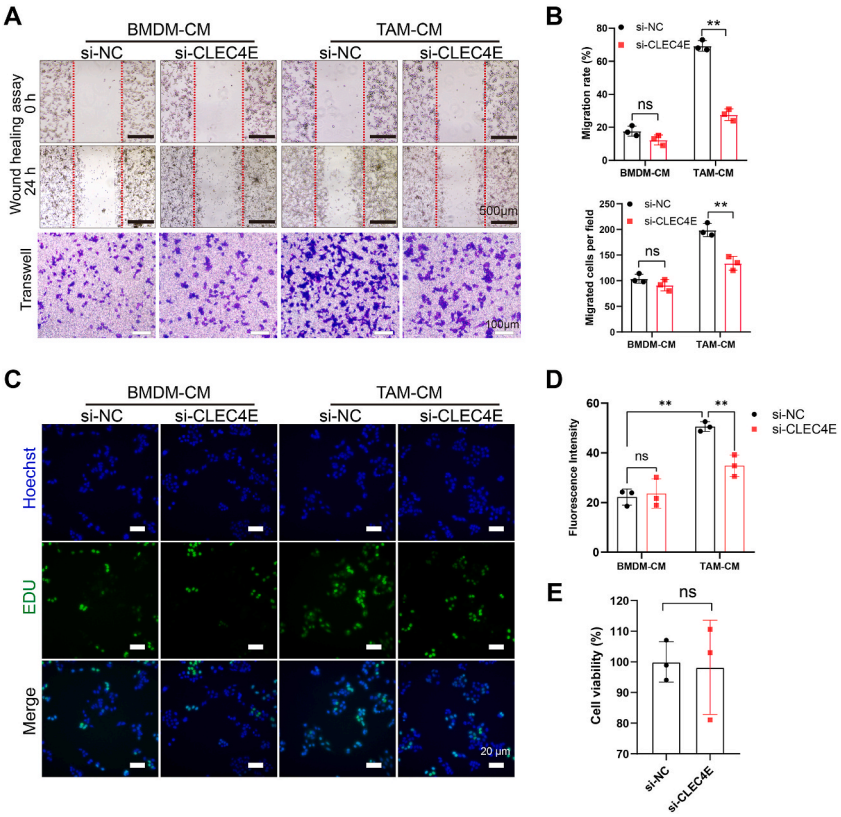

Fig. 5. CLEC4E was essential for the pro-tumoral effects of TAMs. (**A, B**) Wound healing and transwell invasion assays of MFC under stimulation with or without conditioned medium obtained from MFC-CM stimulated BMDMs pretreated with si- NC or si-CLEC4E *in vitro* and quantitative analysis of migration rate and migrated cells (n = 3). (**C**) EDU staining in indicated groups and (**D**) quantitative analysis of fluorescence intensity (n = 3). (**E**) Quantitative analysis of MFC viability detected by CCK8 (n = 3). Data represented by mean ± SD. *p < 0.05, **p < 0.01, ns indicates no significance.

CLEC4E resulted in a significant enrichment of genes involved in immune response-related processes, such as leukocyte/lymphocyte-mediated immunity, humoral immune response, and activation of the immune response. Conversely, the negatively coexpressed genes were significantly enriched in epidermal development, keratinocyte differentiation, and cell-cell junction assembly. KEGG results showed that cytokine-cytokine receptor interactions, chemokine signaling pathways, and toll-like receptor signaling pathways were significantly and positively associated with CLEC4E, whereas pathways involved in pancreatic/gastric acid secretion, protein digestion, and absorption were negatively associated with CLEC4E. The GSEA results showed that the adaptive immune system and chemokine signaling pathways were significantly upregulated in the high CLEC4E group (NES >1, NOM p-val <0.05, FDR q-val <0.1) (Fig. 2C and D). The top 10 genes that positively and negatively correlated with CLEC4E expression in GC are shown in (Fig. 2E and F). In addition, the gene-gene interaction network for CLEC4E constructed using GeneMania further confirmed that genes closely correlated with CLEC4E were significantly related to the regulation of the innate immune response (Fig. 2G). Collectively, these results demonstrate that CLEC4E is involved in the immune response in the TME of GC and that CLEC4E may contribute to gastric carcinogenesis by affecting cell differentiation.

3.3. Upregulated expression of CLEC4E was significantly correlated with infiltrating immune cells in GC

Analysis of tumor-infiltrating immune cells in GC correlated with CLEC4E expression was conducted using the TIMER database. The results showed a significant positive correlation between CLEC4E expression and the infiltration of $CD8^+$ T cells, macrophages, neutrophils, and dendritic cells, whereas the infiltration of $CD4^+$ T cells was not significantly correlated (Fig. 3A). Using the GSVA package and the established ssGSEA algorithm, we further estimated the correlation between CLEC4E and the infiltration of 24 immune cell types in GC. We found that the expression of CLEC4E had significant positive correlation with multiple immune cell infiltrations in GC, especially the infiltration levels of macrophages, which was consistent with the results of the TIMER database (Fig. 3B). To explore whether CLEC4E affects GC prognosis by altering immune infiltration, we performed prognostic analyses based on CLEC4E expression in GC with relevant immune cell subtypes. As shown in Fig. 3C–D, GC patients with high expression of CLEC4E and reduced infiltration of $CD4^+$ T cells, $CD8^+$ T cells, and NK cells, as well as an increased number of regulatory T cells, demonstrated a poor prognosis. These results indicate that CLEC4E significantly affects immune cell infiltration in the TME, which may in part affect

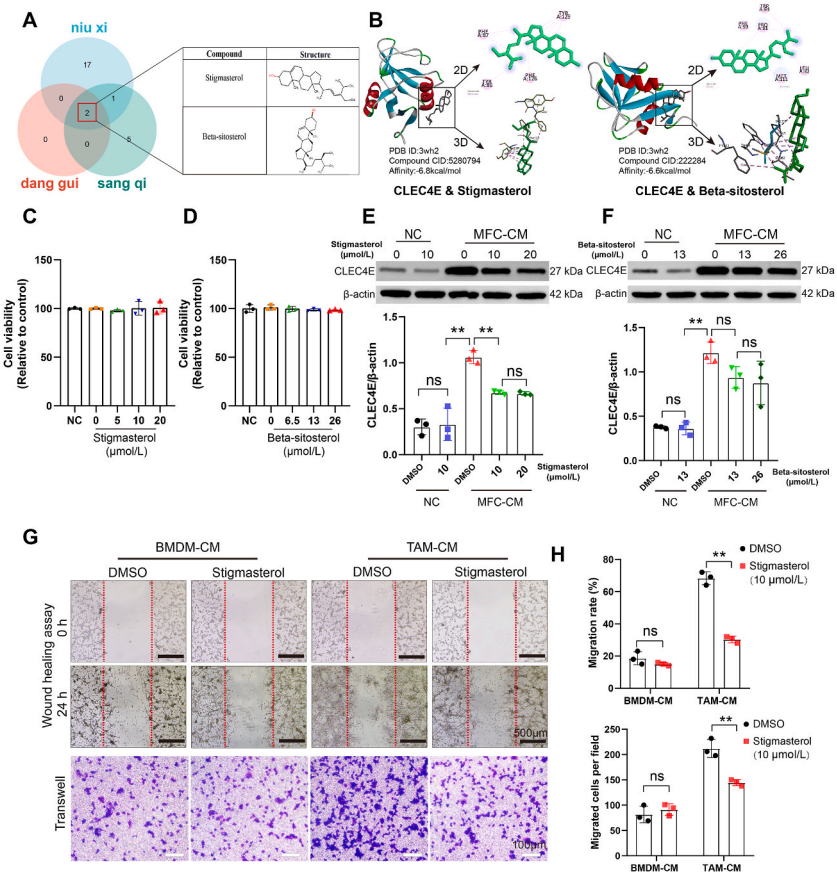

Fig. 6. Stigmasterol targeted CLEC4E in TAMs to inhibit GC progression. (**A**) Venn diagram of compounds with potential effects on CLEC4E for the treatment of GC. (**B**) The docking mode of CLEC4E (PDB ID: 3wh2) with Stigmasterol or Beta-sitosterol separately. (**C–D**) Cell viability detected by CCK8 and quantitative analysis of BMDMs (n = 3). (**E-F**) Western blot of CLEC4E in Stigmasterol or Beta-sitosterol pretreated BMDMs with or without MFC-CM treatment, respectively, and quantitative analysis (n = 3). The original blots are shown in Supplementary Figs. S3A–B. (**G-H**) Wound healing and transwell invasion assays of MFC under stimulation with conditioned medium obtained from MFC-CM stimulated BMDMs pretreated with DMSO or Stigmasterol (10 μmol/L), and quantitative analysis of migration rate and migrated cells (n = 3). Data represented by mean ± SD. *p < 0.05, **p < 0.01, ns indicates no significance.

the prognosis of patients with GC.

3.4. TME induced CLEC4E expression in TAMs to mediate cancer progression

Because of cellular heterogeneity in GC tissues, we analyzed a scRNA-seq dataset derived from the publicly available GEO database (GSM5004181, https://www.ncbi.nlm.nih.gov/geo/). Interestingly, the results showed that CLEC4E was predominantly expressed in myeloid cells, which are the main source of macrophages (Tumor-Associated Macrophages, TAMs) in the gastrointestinal tract [23,24] (Fig. 4A). Immunofluorescent staining of CLEC4E and CD68 in normal human gastric tissue and GC tissue showed that positive CLEC4E cells colocalized with $CD68^{+}$ macrophages, which confirmed the scRNA-seq results (Fig. 4B–D). As one of the predominant stromal cell types in the TME, TAMs are affected by cancer cell-derived cytokines [25]. Given the 97% peptide sequence homology between human and mouse CLEC4E (E = 5e-101), as determined by NCBI BLAST (https://blast.ncbi.nlm.nih.gov/Blast.cgi) analysis, we conducted *in vitro* experiments using MFC. To investigate whether the TME affected CLEC4E expression in TAMs, BMDMs were obtained and stimulated with 10% MFC-conditioned medium (MFC-CM), and the TAM-CMs were subsequently collected (Fig. 4E). Western blotting results showed that MFC-CM significantly increased the protein levels of CLEC4E in BMDMs (Fig. 4F). To examine the functional role of CLEC4E, si-RNAs (si-CLEC4E1-3) were employed to perform the loss-of-function studies (Fig. 4G). As shown in Fig. 4H–I, si-CLEC4E1 showed the highest knockdown efficiency and significantly suppressed the upregulation of CLEC4E induced by MFC-CM, then it was used in subsequent experiments. As revealed by the wound healing and invasion assays in Fig. 5A–B, the migration and invasion of MFC was markedly enhanced when stimulated by the 50% conditioned medium of BMDMs pro-stimulated by MFC-CM (TAM-CM) compared to that of the50% normal conditioned medium (BMDM-CM) groups while stable silencing the expression of CLEC4E significantly hampered these effects. EdU staining demonstrated that TAM-CM facilitated MFC proliferation. Knockdown of CLEC4E by siRNA in BMDMs weakened the pro-tumoral effects on MFC induced by the TAM-CM (Fig. 5C and D). Moreover, silencing CLEC4E

expression in MFC did not affect their viability (Fig. 5E). These results illustrate that CLEC4E is predominantly expressed in TAMs in GC and that the TME can induce CLEC4E expression to mediate tumor progression.

3.5. Prediction of drugs targeting CLEC4E to inhibit cancer progression

Based on Coremine medical database mining, 10 kinds of TCMs with potential effects on CLEC4E were identified. Three of these drugs, niu xi, dang gui, and san qi, are included in the Chinese Pharmacopoeia (2020 edition). After obtaining 20, 2, and 8 active ingredients from these three herbs from the TCMSP online database, two potential therapeutic compounds (Stigmasterol and Beta-sitosterol) were identified by intersection (Fig. 6A). The molecular docking results showed that Stigmasterol and Beta-sitosterol could bind to CLEC4E with high affinity, and the binding free energy were −6.8 and −6.6 kcal/mol respectively (Fig. 6B). To test the inhibitory effects of Stigmasterol and Beta-sitosterol on cancer cells through TAMs, different concentrations were used as described in previous studies [26,27]. Initially, the CCK-8 kit was used to conduct a cell cytotoxicity assay to test the effects of Stigmasterol and Beta-sitosterol on BMDMs. The results showed that 0–20 μmol/L of stigmasterol and 0–26 μmol/L of Beta-sitosterol had no effects on the cell viability (Fig. 6C–D). As expected, stigmasterol, but not beta-sitosterol, significantly decreased the CLEC4E levels in BMDMs stimulated with MFC-CM compared with the DMSO control group (Fig. 6E–F). Meanwhile, treatment of BMDMs with stigmasterol (10 μmol/L) significantly inhibited the pro-migration and pro-invasion effects of MFC cancer cells induced by TAM-CM similar to the effects observed with si-CLEC4E (Fig. 6G and H). These findings indicate that CLEC4E in TAMs is a new therapeutic target for GC and stigmasterol may be a potential therapeutic drug specifically targeting CLEC4E.

4. Discussion

In this study, we validated that CLEC4E was significantly upregulated in GC and that its expression was negatively correlated with patient prognosis. Further analysis demonstrated that CLEC4E was closely correlated with immune cell infiltration and was predominantly expressed in TAMs to mediate GC progression, which can be specifically targeted by si-CLEC4E or the small-molecule stigmasterol. Collectively, CLEC4E is a potential prognostic biomarker and new therapeutic target for GC that can be specifically targeted by stigmasterol.

Inflammation is an important component of tumor progression, and many cancers are caused by infection, chronic stimulation, and inflammation [28]. Studies have shown that the inflammatory microenvironment promotes tumor cell proliferation, survival, and migration, and is an indispensable part of tumor occurrence and development [29,30]. The damage caused by inflammation-induced DNA mutations accounts for approximately 25% of all carcinogenic factors [31]. Studies have shown that *Helicobacter pylori* infection can activate gastric mucosal inflammation through the TLR2/NLRP3/caspase-1/IL-18 pathway, leading to the occurrence of GC [32]. CLEC4E is involved in the activation of the NF-κB inflammatory pathway and the formation of TME [12,13,33]. In this study, we observed that the expression of CLEC4E increased as GC progressed, significantly affecting immune cell infiltration, and was negatively correlated with prognosis. This observation is consistent with previous research showing that CLEC4E possesses pro-tumoral activities and is essential for lung cancer progression.[16]

The TME is composed of multiple components, including TAMs, which can interact with cancer cells to facilitate tumor proliferation and angiogenesis [34,35]. TAMs play important roles in cancer-related inflammation and tumor immunity [36] as well as treatment resistance [25]. Depending on the source, TAMs in the gastrointestinal tract are mainly myeloid-derived, enter the intestine through the bloodstream and settle there [23]. Generally, TAMs are thought to be involved in innate immunity and enhance the tumor immune response [37]. However, several studies have demonstrated controversial results showing that TAMs promote cancer progression and metastasis [38]. It has been reported that activated TAMs can produce IL-10, TGF-β, prostaglandin E2, and the programmed death-ligand 1 to attenuate the inflammation of the TME in GC [39,40]. These studies indicate that TAM-targeting strategies may be effective in the prevention and treatment of patients with GC. Interestingly, our scRNA-seq results in GC demonstrated that, TAM are one of the major components of infiltrating leukocytes, consistent with previous reports [38,41]. Coincidentally, CLEC4E was predominantly expressed in TAMs in GC, as verified using clinical specimens and *in vitro* experiments. We found that targeting TAMs with siRNA or small-molecule compounds to specifically inhibit CLEC4E expression significantly inhibited cancer cell proliferation, migration, and invasion, further confirming previous conclusions.

Currently, treatment strategies for GC mainly include surgery, chemotherapy and molecular targeting therapy. However, the therapeutic results are still disappointing [42]. TCM has gained favor for the treatment of cancers owing to its multiple targets and possible direct or indirect synergistic effects [43,44]. Stigmasterol and Beta-sitosterol are natural phytosterol compounds with multiple biological activities including antioxidant, anti-inflammatory, anticancer, and cholesterol-lowering effects [26,45]. Stigmasterol exerts its anti-tumor effects by inhibiting tumor cell proliferation, invasion, metastasis, and neovascularization [46]. Stigmasterol induces apoptosis and reduces cell proliferation to exert therapeutic effects on breast tumor [47]. Using bioinformatics analysis and network pharmacology, we predicted and confirmed that stigmasterol targets CLEC4E in TAMs to indirectly inhibit cancer progression. These results shed new light on the application of stigmasterol as a novel candidate for the treatment of GC.

A limitation of this study was that further mouse models with transplanted tumors were not constructed to confirm the function of CLEC4E and the anti-tumor effects of stigmasterol in vivo was not assessed. Whether upregulated CLEC4E in TAMs can induce the polarization of TAMs in GC to promote tumor progression, as previously described lung carcinoma [16], needs to be further explored. Additionally, the therapeutic mechanism of targeting CLEC4E requires further investigation to make it suitable for clinical application.

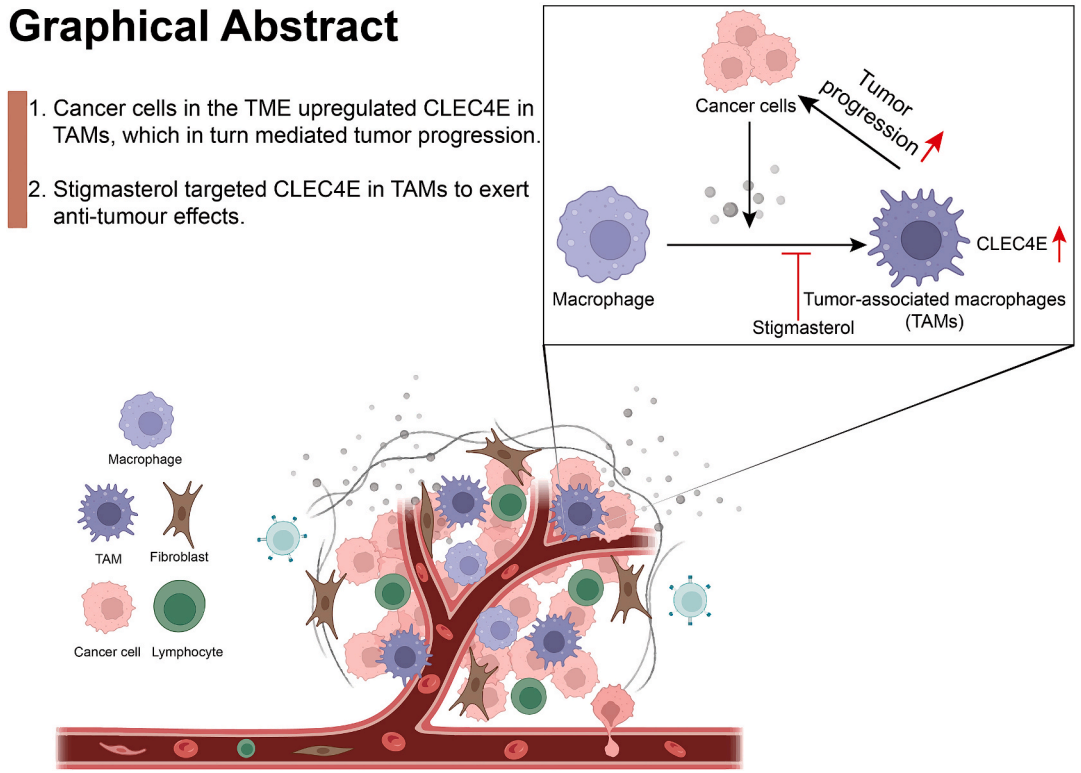

Fig. 7. Graphical illustration of the therapeutic role of CLEC4E. The tumor microenvironment (TME) of GC upregulated the expression of CLEC4E in tumor-associated macrophages (TAMs), which in turn mediated tumor progression. Stigmasterol treatment could targeted CLEC4E specifically in TAMs to indirectly inhibit cancer progression. Created in BioRender (https://biorender.com/).

5. Conclusion

As illustrated in Fig. 7, CLEC4E was significantly upregulated and predominantly expressed in TAMs in GC. Specifically targeting CLEC4E in TAMs with stigmasterol inhibited the proliferation, migration, and invasion of GC tumor cells. This study provides novel insights for the prevention of GC and introduces a new strategy for the treatment of patients with GC.

Ethics statement

The study was reviewed and approved by the Ethics Committee of the Sixth Hospital of Wuhan (CREC Ref. No: WHSHIRB-K-2023010). Animal experiments were performed comply with all regulations of the Chinese Council on Animal Care and written informed consent was obtained from all patients participated in the study.

Data availability

The data are available from the corresponding author upon reasonable request.

CRediT authorship contribution statement

Qin Jiang: Conceptualization, Methodology, Visualization, Writing – original draft. **Dan Xiao:** Data curation, Investigation. **Ao Wang:** Data curation, Investigation. **Qiong Yu:** Methodology, Software. **Ying Yin:** Methodology, Software. **Jingchong Wu:** Investigation, Resources. **Yan Zhang:** Investigation, Resources. **Tian Jin:** Methodology. **Baicheng Kuang:** Data curation, Methodology, Visualization, Writing – review & editing. **Yegui Jia:** Conceptualization, Funding acquisition, Resources, Writing – review & editing.

Declaration of competing interest

The authors declare that they have no known competing financial interests or personal relationships that could have appeared to influence the work reported in this paper.

Acknowledgements

The present study was supported by the scientific research projects of the Chinese Medicine Administrative Bureau of Hubei Province (no. ZY2023F065).

Appendix A. Supplementary data

Supplementary data to this article can be found online at https://doi.org/10.1016/j.heliyon.2024.e27172.

References

[1] A.P. Thrift, H.B. El-Serag, Burden of gastric cancer, Clin. Gastroenterol. Hepatol. 18 (3) (2020) 534–542.
[2] E.C. Smyth, M. Nilsson, H.I. Grabsch, et al., Gastric cancer, Lancet 396 (10251) (2020) 635–648.
[3] H. Sung, J. Ferlay, R.L. Siegel, et al., Global cancer statistics 2020: GLOBOCAN estimates of incidence and mortality worldwide for 36 cancers in 185 countries, CA A Cancer J. Clin. 71 (3) (2021) 209–249.
[4] C. Allemani, H.K. Weir, H. Carreira, et al., Global surveillance of cancer survival 1995-2009: analysis of individual data for 25,676,887 patients from 279 population-based registries in 67 countries (CONCORD-2), Lancet 385 (9972) (2015) 977–1010.
[5] H. Katai, T. Ishikawa, K. Akazawa, et al., Five-year survival analysis of surgically resected gastric cancer cases in Japan: a retrospective analysis of more than 100,000 patients from the nationwide registry of the Japanese Gastric Cancer Association (2001-2007), Gastric Cancer 21 (1) (2018) 144–154.
[6] Z. Tan, Recent advances in the surgical treatment of advanced gastric cancer: a review, Med. Sci. Mon. Int. Med. J. Exp. Clin. Res. 25 (2019) 3537–3541.
[7] D. Zeng, M. Li, R. Zhou, et al., Tumor microenvironment characterization in gastric cancer identifies prognostic and immunotherapeutically relevant gene signatures, Cancer Immunol. Res. 7 (5) (2019) 737–750.
[8] B. Zhang, Q. Wu, B. Li, et al., m(6)A regulator-mediated methylation modification patterns and tumor microenvironment infiltration characterization in gastric cancer, Mol. Cancer 19 (1) (2020) 53.
[9] R. Noy, J.W. Pollard, Tumor-associated macrophages: from mechanisms to therapy, Immunity 41 (1) (2014) 49–61.
[10] X. Xiong, X. Xie, Z. Wang, et al., Tumor-associated macrophages in lymphoma: from mechanisms to therapy, Int. Immunopharm. 112 (2022) 109235.
[11] T.B. Geijtenbeek, S.I. Gringhuis, Signalling through C-type lectin receptors: shaping immune responses, Nat. Rev. Immunol. 9 (7) (2009) 465–479.
[12] L.M. Kingeter, X. Lin, C-type lectin receptor-induced NF-κB activation in innate immune and inflammatory responses, Cell. Mol. Immunol. 9 (2) (2012) 105–112.
[13] X. Lu, M. Nagata, S. Yamasaki, Mincle: 20 years of a versatile sensor of insults, Int. Immunol. 30 (6) (2018) 233–239.
[14] L.L. Lv, P.M. Tang, C.J. Li, et al., The pattern recognition receptor, Mincle, is essential for maintaining the M1 macrophage phenotype in acute renal inflammation, Kidney Int. 91 (3) (2017) 587–602.
[15] Y. Zhang, H. Wei, L. Fan, et al., CLEC4s as potential therapeutic targets in hepatocellular carcinoma microenvironment, Front. Cell Dev. Biol. 9 (2021) 681372.
[16] C. Li, V.W. Xue, Q.M. Wang, et al., The mincle/syk/NF-kappaB signaling circuit is essential for maintaining the protumoral activities of tumor-associated macrophages, Cancer Immunol. Res. 8 (8) (2020) 1004–1017.
[17] T. Li, J. Fu, Z. Zeng, et al., TIMER2.0 for analysis of tumor-infiltrating immune cells, Nucleic Acids Res. 48 (W1) (2020) W509–w514.
[18] M.J. Goldman, B. Craft, M. Hastie, et al., Visualizing and interpreting cancer genomics data via the Xena platform, Nat. Biotechnol. 38 (6) (2020) 675–678.
[19] A. Guo, J. Zhang, Y. Tian, et al., Identify the immune characteristics and immunotherapy value of CD93 in the pan-cancer based on the public data sets, Front. Immunol. 13 (2022) 907182.
[20] Y. Yoshimatsu, S. Kimuro, J. Pauty, et al., TGF-beta and TNF-alpha cooperatively induce mesenchymal transition of lymphatic endothelial cells via activation of Activin signals, PLoS One 15 (5) (2020) e0232356.
[21] Z. Zou, R. Shang, L. Zhou, et al., The Novel MyD88 Inhibitor TJ-M2010-5 Protects against Hepatic Ischemia-Reperfusion Injury by Suppressing Pyroptosis in Mice, Transplantation, 2022.
[22] C.R. Justus, N. Leffler, M. Ruiz-Echevarria, et al., In vitro cell migration and invasion assays, J. Vis. Exp. 88 (2014).
[23] C.C. Bain, A.M. Mowat, Macrophages in intestinal homeostasis and inflammation, Immunol. Rev. 260 (1) (2014) 102–117.
[24] T.C. Moreira Lopes, D.M. Mosser, R. Gonçalves, Macrophage polarization in intestinal inflammation and gut homeostasis, Inflamm. Res. 69 (12) (2020) 1163–1172.
[25] E. Van Overmeire, D. Laoui, J. Keirsse, et al., Mechanisms driving macrophage diversity and specialization in distinct tumor microenvironments and parallelisms with other tissues, Front. Immunol. 5 (2014) 127.
[26] H. Bae, G. Song, W. Lim, Stigmasterol causes ovarian cancer cell apoptosis by inducing endoplasmic reticulum and mitochondrial dysfunction, Pharmaceutics 12 (6) (2020).
[27] Z. Wang, Y. Zhan, J. Xu, et al., Beta-sitosterol reverses multidrug resistance via BCRP suppression by inhibiting the p53-MDM2 interaction in colorectal cancer, J. Agric. Food Chem. 68 (12) (2020) 3850–3858.
[28] H.E. Sabaawy, B.M. Ryan, H. Khiabanian, et al., JAK/STAT of all trades: linking inflammation with cancer development, tumor progression and therapy resistance, Carcinogenesis 42 (12) (2021) 1411–1419.
[29] L.M. Coussens, Z. Werb, Inflammation and cancer, Nature 420 (6917) (2002) 860–867.
[30] R. Khandia, A. Munjal, Interplay between inflammation and cancer, Adv. Protein Chem. Struct. Biol. 119 (2020) 199–245.
[31] M. Murata, Inflammation and cancer, Environ. Health Prev. Med. 23 (1) (2018) 50.
[32] K.N. Koch, A. Müller, Helicobacter pylori activates the TLR2/NLRP3/caspase-1/IL-18 axis to induce regulatory T-cells, establish persistent infection and promote tolerance to allergens, Gut Microb. 6 (6) (2015) 382–387.
[33] S. Zhou, Y. Sun, T. Chen, et al., The landscape of the tumor microenvironment in skin cutaneous melanoma reveals a prognostic and immunotherapeutically relevant gene signature, Front. Cell Dev. Biol. 9 (2021) 739594.
[34] S. Su, Q. Liu, J. Chen, et al., A positive feedback loop between mesenchymal-like cancer cells and macrophages is essential to breast cancer metastasis, Cancer Cell 25 (5) (2014) 605–620.
[35] C. Engblom, C. Pfirschke, M.J. Pittet, The role of myeloid cells in cancer therapies, Nat. Rev. Cancer 16 (7) (2016) 447–462.
[36] L. Cassetta, S. Fragkogianni, A.H. Sims, et al., Human tumor-associated macrophage and monocyte transcriptional landscapes reveal cancer-specific reprogramming, biomarkers, and therapeutic targets, Cancer Cell 35 (4) (2019) 588–602.e10.
[37] Y. Chen, Y. Song, W. Du, et al., Tumor-associated macrophages: an accomplice in solid tumor progression, J. Biomed. Sci. 26 (1) (2019) 78.
[38] V. Gambardella, J. Castillo, N. Tarazona, et al., The role of tumor-associated macrophages in gastric cancer development and their potential as a therapeutic target, Cancer Treat Rev. 86 (2020) 102015.
[39] T. Kitamura, B.Z. Qian, J.W. Pollard, Immune cell promotion of metastasis, Nat. Rev. Immunol. 15 (2) (2015) 73–86.
[40] A. Mantovani, A. Vecchi, P. Allavena, Pharmacological modulation of monocytes and macrophages, Curr. Opin. Pharmacol. 17 (2014) 38–44.
[41] G. Zhang, Z. Gao, X. Guo, et al., CAP2 promotes gastric cancer metastasis by mediating the interaction between tumor cells and tumor-associated macrophages, J. Clin. Invest. 133 (21) (2023).

[42] Z. Cheng, G. Liu, C. Huang, et al., Upregulation of circRNA_100395 sponges miR-142-3p to inhibit gastric cancer progression by targeting the PI3K/AKT axis, Oncol. Lett. 21 (5) (2021) 419.
[43] X. Li, G. Yang, X. Li, et al., Traditional Chinese medicine in cancer care: a review of controlled clinical studies published in Chinese, PLoS One 8 (4) (2013) e60338.
[44] G. Yang, X. Li, X. Li, et al., Traditional Chinese medicine in cancer care: a review of case series published in the Chinese literature, Evid. Based Complement. Alternat. Med. (2012) 751046, 2012.
[45] S. Bakrim, N. Benkhaira, I. Bourais, et al., Health benefits and pharmacological properties of stigmasterol, Antioxidants 11 (10) (2022).
[46] K. Li, D. Yuan, R. Yan, et al., Stigmasterol exhibits potent antitumor effects in human gastric cancer cells mediated via inhibition of cell migration, cell cycle arrest, mitochondrial mediated apoptosis and inhibition of JAK/STAT signalling pathway, J. BUON 23 (5) (2018) 1420–1425.
[47] M. AmeliMojarad, M. AmeliMojarad, A. Pourmahdian, The inhibitory role of stigmasterol on tumor growth by inducing apoptosis in Balb/c mouse with spontaneous breast tumor (SMMT), BMC Pharmacol Toxicol 23 (1) (2022) 42.